$$T\Delta S(1, \text{classical}) = 13.3 \pm 0.4$$

$$T\Delta S(2, \text{quantum}) = 11.3 \pm 0.4$$

$$T\Delta S(2, \text{classical}) = 12.4 \pm 0.4$$

where 1 and 2 denote peptides 1 and 2, respectively, and $T = 307.9$ K; the quantum and classical refer to results obtained by eqs 48 and 49, respectively. These results show a difference of ~ 1 kcal/mol between the corresponding results for peptides 1 and 2. The values of ΔS(classical) are always larger by ~ 1 kcal/mol than the corresponding quantum mechanical values. The above results, as a whole, are 2–4 kcal/mol larger than the value of 9.4 obtained by the local states method. It should be pointed out again that our elimination of the contribution of only six frequencies for the peptides in the crystal is somewhat arbitrary since nonzero components of translation and rotation were found to exist for other frequencies as well (notice that elimination of additional frequencies would lower the values of ΔS).

For the peptide in vacuum we have calculated the entropy for several other minimum energy conformations accessible to the molecule. The difference between the maximum and minimum values found for the quantum mechanical entropy (TS, eq 48) was 1.5 kcal/mol. Also, in the calculations described above of S_p^A(cell) for the peptide in the crystal, the data from both peptides were used together to obtain a single value of the entropy (Table IV). We have calculated tables similar to Tables I and IV for the peptides 1 and 2 separately. The corresponding values of $\Delta\alpha_k$ are obviously smaller than those based on the two peptides together, and thus the values of $T\Delta S^A$ are up to 1 kcal/mol larger than those of Table IV, but they are still smaller than those obtained with the harmonic approximations.

IV. Summary

The LS method is general in the sense that it is not limited to handling the entropy of harmonic or quasiharmonic conformational changes but can be applied to any chain flexibility (see ref 37). The method provides approximations for the entropy which can be systematicly improved by increasing the correlation and discretization parameters, b and l, respectively.

Here the LS method was applied to samples obtained from molecular dynamics simulations of cyclo-(Ala-Pro-D-Phe)$_2$ in vacuum and in the crystal. The free energy functionals F^B (eq 21) and F^A (eq 18) and the fluctuation $\sigma_F{}^A$ (eq 29) of the latter were calculated (F^B was only calculated for the peptide in vacuum) and shown to satisfy certain theoretical relations, which suggests that the method is reliable. In the usual application of the LS method to a chain in vacuum, one would seek to estimate $F^M = (F^A + F^B)/2$, which is expected to provide the best approximation for the correct free energy, F. However, this might require generating relatively large samples in order to adequately estimate F^B. Also, for a peptide in solvent or in the crystal, F^B for the peptide chain is not well defined. Therefore, in such cases one can only calculate S^A (or some approximations F^A) and the difference ΔS^A (ΔF^A) between the S^A (F^A) values of two different conformational states. An important conclusion is that in certain cases the results for $\Delta F^A(b,l)$ and $\Delta S^A(b,l)$ converge rapidly at small values of b and l, which suggests that these functionals provide very good approximations for the correct ΔF and ΔS, respectively. The computational advantage of using F^A and S^A rather than F^B lies in the fact that they can be estimated efficiently from relatively small samples. Furthermore, if the ranges of the angle–angle correlations (measured by b) of two states are comparable and the corresponding values of $\Delta\alpha_k$ are not extremely different, the worst approximation, which ignores correlations and assumes homogeneous distribution of angles ($b = 0$, $l = 1$), provides a reasonable estimate of the correct ΔF (and ΔS). This is also important since the above approximation requires the minimal number of local states K' (i.e., the total number of angles), and therefore relatively small samples and very little computer memory are needed; thus, it can be applied efficiently to proteins of any size.

The LS method could be used (together with the appropriate energy contributions) to compare *approximately* the free energy of binding of various ligands to a protein, where at this stage the contribution of solvent entropy is ignored.[3] However, in principle, the entropy of diffusive systems such as a fluid can also be calculated with the LS method, since it was originally developed for Ising and lattice gas models.[31–33] This is planned for future work.

Acknowledgment. We thank Dr. Rick Fine for helpful discussions. This work was supported in part by grants from the National Institutes of Health (Grants GM30564 and GM45651) by the Supercomputer Computations Research Institute which is supported in part by the U.S. Department of Energy through Contract No. DE-FC05-85ER250000. Computer time was provided by the San Diego Supercomputer Center (SDSC) on the Cray X-MP/48 and Y-MP8/864.

Registry No. Cyclo-(Ala-Pro-D-PHE)$_2$, 52634-26-1.

Ab Initio Studies of Fundamental Cluster Rearrangement Mechanisms

David J. Wales* and Richard G. A. Bone

Contribution from the University Chemical Laboratories, Lensfield Road, Cambridge CB2 1EW, UK. *Received December 16, 1991*

Abstract: Two fundamental cluster rearrangement mechanisms are investigated by ab initio calculations, namely the single diamond-square-diamond (DSD) process in $B_8H_8^{2-}$ and the square-diamond-diamond-square (SDDS) process in $C_5H_5^+$. Geometry optimizations and frequencies are compared for the SCF and second-order Møller–Plesset (MP2) approximations with basis sets ranging in size from STO-3G to double-ζ plus polarization (DZP). The results are in good agreement with expectations, especially orbital symmetry selection rules, and enable us to compare the effects of electron correlation and polarization functions upon the energy and the character of the stationary points. The topology of the potential energy surface of $C_5H_5^+$ is studied in detail, demonstrating that the SDDS mechanism allows all versions of the structure to be accessed.

I. Introduction

In 1966 Lipscomb first proposed the diamond-square-diamond (DSD) process to account for rearrangements in boranes and carboranes.[1] This mechanism is a cornerstone of recent theoretical developments based upon Stone's Tensor Surface Harmonic (TSH) theory which have provided powerful general orbital symmetry selection rules for such processes.[2–5] These theories

(1) Lipscomb, W. N. *Science* **1966**, *153*, 373.

(2) Wales, D. J.; Stone, A. J. *Inorg. Chem.* **1987**, *26*, 3845.

(3) Wales, D. J.; Mingos, D. M. P.; Lin, Z. *Inorg. Chem.* **1989**, *28*, 2754.

0002-7863/92/1514-5399$03.00/0

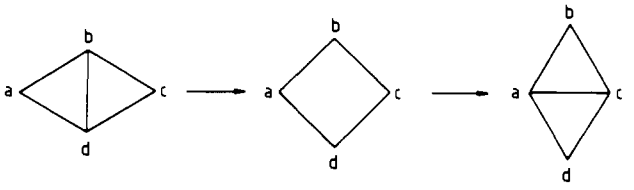

Figure 1. Scheme showing the diamond-square-diamond (DSD) process.

have now been extended to transition-metal and *nido* clusters,[3,5] where new skeletal rearrangement mechanisms must also be considered, such as the square-diamond-diamond-square (SDDS) process. The DSD and SDDS processes will be described in detail in the next section.

The TSH theory approach enables cluster rearrangement processes that are "forbidden" in the Woodward–Hoffmann sense[6] due to orbital crossings to be identified very easily, usually by inspection. The first application of the method to *closo*-boranes and carboranes enabled all the existing experimental data for cage fluxionalities to be understood,[2] and the subsequent applications to more exotic systems led to a number of predictions, some of which are still to be tested by experiment. For example, the SDDS mechanism is expected to be the most favorable rearrangement pathway in systems such as $C_5H_5^+$. However, ab initio calculations including the effects of electron correlation and polarization basis functions have yet to be reported for either of the DSD or SDDS mechanisms. This is the principal aim of the present paper, where we characterize the archetypal symmetry-allowed DSD and SDDS rearrangements in $B_8H_8^{2-}$ and $C_5H_5^+$, respectively.

Lipscomb and co-workers have previously reported a number of studies of the effects of electron correlation and polarization functions in borohydride compounds,[7-12] especially in connection with pyrolysis reaction pathways. For example, the ground-state structure of triborane, B_3H_9, which is probably an important intermediate in the pyrolysis of diborane, is very sensitive to correlation.[12] The electronic contribution to the dissociation energy of diborane is also rather different at the SCF and correlated levels of theory,[10] and both correlation and the inclusion of polarization basis functions change the relative stabilities of various B_4H_{10} structures.[8] Results for B_2H_4 and BH_5 indicate that the relative effects of polarization functions and correlation corrections are additive to a good approximation.[9] However, although certain high energy double DSD processes have been studied in carboranes,[13] the fundamental low energy DSD and SDDS processes have not been accurately characterized before in terms of transition-state calculations. Neither species has any bridging hydrogen atoms, and, of course, the rearrangements considered are nondissociative, so our results provide some interesting comparisons with the previous calculations. In particular, we anticipate that polarization functions may be especially important for $B_8H_8^{2-}$ with a double negative charge. In the next section we review the DSD and SDDS mechanisms and explain why they are of such importance in cluster chemistry.

II. DSD and SDDS Mechanisms

The DSD Process. In the DSD process (Figure 1) an edge common to two triangular faces of a cluster skeleton breaks and a new edge is formed perpendicular to it. DSD rearrangements, or combinations of several concerted DSD processes, have been proposed to rationalize fluxional processes and isomerizations of boranes, carboranes, and metalloboranes.[14,15] King[16] used topological considerations to distinguish between inherently rigid clusters (which contain no degenerate edges) and molecules for which one or more DSD processes are geometrically possible. An edge is said to be degenerate if a DSD rearrangement in which it is broken leads back to the same cluster skeleton, where atoms of the same element are not distinguished. For example, the three equatorial edges of trigonal-bipyramidal $B_5H_5^{2-}$ are degenerate and the others are not. For a degenerative DSD rearrangement to be geometrically possible the connectivities of the new cluster vertices must match those of the original skeleton; in the *closo*-borane series only $B_5H_5^{2-}$, $B_8H_8^{2-}$, $B_9H_9^{2-}$, and $B_{11}H_{11}^{2-}$ satisfy these requirements. King's approach was partially successful in that all the structures he predicted to be rigid are found experimentally to be nonfluxional. However, some of the above molecules in the $B_nH_n^{2-}$ series with topologically possible single DSD rearrangements are not fluxional on the NMR time scale. They are the ones that have $4p + 1$ vertex atoms.

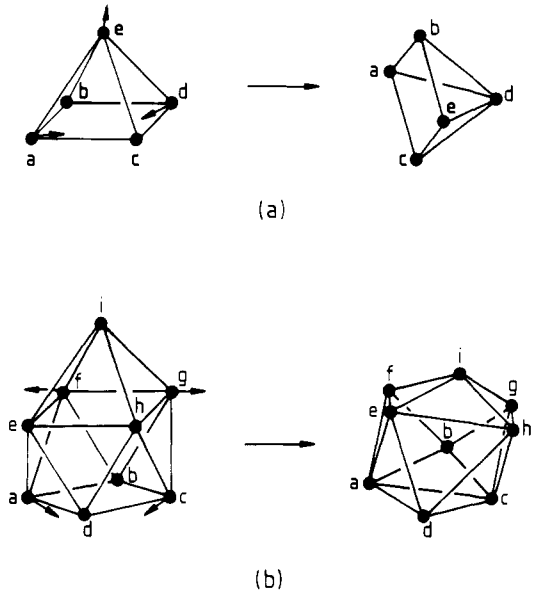

Figure 2. Scheme showing the square → diamond, diamond → square (SDDS) mechanism for a square-based pyramid (a) and a capped square antiprism (b).

Stone's TSH theory[5,17] enables us to explain why the DSD process is so favorable and provides a framework for the derivation of some powerful orbital symmetry selection rules. For example, we can show that transition states for *closo*-boranes or carboranes with a single atom on a principal rotation axis of order ≥3 generally have an orbital crossing.[2] These results may be extended to show that an orbital crossing will generally result if a mirror plane through the critical face is retained throughout the process.[3] If a C_2 axis is retained, however, then there is an avoided crossing and the process is "allowed". Using the above rules, and the additional criterion that multiple DSD processes are likely to be less favorable than the single DSD process, it is possible to rationalize the whole range of rearrangement rates of the *closo*-boranes and carboranes.[2] We have also discussed the application of the rules to rearrangements of transition-metal clusters and suggested some new mechanisms for these species.[3] Second-order Jahn–Teller analysis supports the selection rules deduced from TSH theory.[4] Previous calculations on $B_8H_8^{2-}$ using the MNDO[18]

(4) Wales, D. J.; Mingos, D. M. P. *Polyhedron* **1989**, *15*, 1933.
(5) Mingos, D. M. P.; Wales, D. J. *Introduction to Cluster Chemistry*; Prentice-Hall: Englewood Cliffs, 1990.
(6) Woodward, R. B.; Hoffmann, R. *Angew Chem., Int. Ed. Engl.* **1969**, *8*, 781.
(7) McKee, M. L.; Lipscomb, W. N. *Inorg. Chem.* **1981**, *20*, 4442.
(8) McKee, M. L.; Lipscomb, W. N. *Inorg. Chem.* **1981**, *20*, 4452.
(9) McKee, M. L.; Lipscomb, W. N. *J. Am. Chem. Soc.* **1981**, *103*, 4673.
(10) Stanton, R. F.; Bartlett, R. J.; Lipscomb, W. N. *Chem. Phys. Lett.* **1987**, *138*, 525.
(11) Stanton, R. F.; Lipscomb, W. N.; Bartlett, R. J. *J. Chem. Phys.* **1988**, *88*, 5726.
(12) Stanton, R. F.; Lipscomb, W. N.; Bartlett, R. J.; McKee, M. L. *Inorg. Chem.* **1989**, *28*, 109.
(13) McKee, M. L. *J. Am. Chem. Soc.* **1988**, *110*, 5317.
(14) Wade, K. *Electron Deficient Compounds*; Nelson: London, 1971.
(15) See, e.g.: Kennedy, J. D. In *Progress in Inorganic Chemistry*; John Wiley: New York, 1986; Vol. 34.
(16) King, R. B. *Inorg. Chim. Acta* **1981**, *49*, 237.
(17) Stone, A. J. *Mol. Phys.* **1980**, *41*, 1339. Stone, A. J.; Alderton, M. J. *Inorg. Chem.* **1982**, *21*, 2297. Stone, A. J. *Polyhedron* **1984**, *3*, 1299.

and PRDDO[19] methods support the theoretical analysis and suggest that there is a bicapped trigonal prismatic transition state of C_{2v} symmetry. A qualitative analysis by Fuller and Kepert leads to the same conclusion.[20]

It is also of interest to note that numerous DSD processes, and combinations thereof, have been identified as true transition states in model inert gas and trapped ion clusters.[21] In such species the cohesive forces that bind the cluster are much easier to describe, and there are no orbital symmetry "forbidden" processes. Hence, King's topological analysis may be applied directly to rationalize the relative fluxionalities of small inert gas and trapped ion clusters. This result has far-reaching implications for the dynamical behavior of such systems, especially for the theory of solid-like/liquid-like coexistence, as we have explained elsewhere.[22]

The SDDS Process. The presence of a single square face in an otherwise deltahedral cluster introduces the possibility of a new low energy rearrangement mechanism. Such a process may be written as a square → diamond, diamond → square or SDDS mechanism. This concerted process is illustrated for the square-based pyramid and the capped square antiprism in Figure 2; we see that there are two critical edges—one is broken and one is made. If a mirror plane which contains one of these edges and is perpendicular to the other is retained throughout, then this mechanism involves two orbital crossings.[3] If the edges are parallel (Figure 2) then there are two avoided crossings and the process is orbital symmetry allowed. There is no TSH symmetry-forced crossing, since the starting and finishing molecules both have a single atom on the 4-fold principal axis. Hence this may be a favorable process for *nido* clusters. For *nido*-boranes, however, the presence of bridging hydrogen atoms around the open face means that this mechanism is not likely to occur. It could, however, be significant in accounting for the behavior of $B_8H_8^{2-}$ in solution[23] where a fluxional bicapped trigonal prismatic geometry may be present. The SDDS mechanism is allowed by orbital symmetry for the latter species and may account for its non-rigidity.

Probably the simplest molecule for which we predict the SDDS process to be favorable is $C_5H_5^+$, which is expected to exhibit a local energy minimum for the *nido* square-based pyramid. The latter structure and our suggested C_{2v} transition state (Figure 3) were considered by Stohrer and Hoffmann in a study of tricyclopentanes.[24] These early semiempirical calculations suggested that the C_{2v} structure is higher in energy than the C_{4v} square-based pyramid, in line with our theoretical expectations. A subsequent study by Bouman et al.[25] coupled permutation-inversion symmetry[26] and group theory with CNDO calculations of energies and derivatives and concluded that the C_{2v} structure is a saddle point of index 3, i.e. not a true transition state.[27] From group theoretical arguments the latter authors also concluded that even if the C_{2v} structure were a transition state, it could not lead to all possible permutational exchanges of vertices. This again contradicts the conclusions of Stohrer and Hoffmann. However, the present work shows that the C_{2v} structure is indeed a true transition state, that the SDDS mechanism for the square-based pyramid is correct, and that if this mechanism is feasible[26] then the effective molecular symmetry group is the complete nuclear permutation-inversion group.

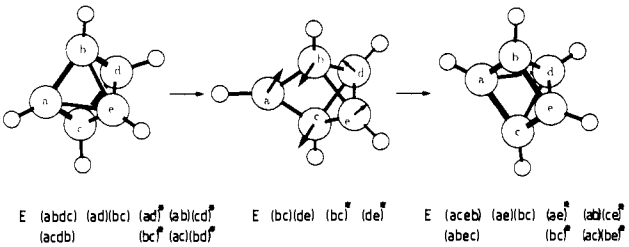

Figure 3. Mechanism of the SDDS process in $C_5H_5^+$. The transition vector corresponding to the normal mode with the imaginary frequency has been sketched for the transition state, and the square faces are highlighted. The labeling is consistent with that shown in Figure 2. The permutation-inversion symmetry operations are listed below each structure. Note that the operation (bc)* (corresponding to the operation of reflection in the plane containing atoms a, e, and d) is conserved throughout.

III. Results and Discussion

We performed symmetry-constrained geometry optimizations in internal coordinates for both $B_8H_8^{2-}$ and $C_5H_5^+$ at each level of theory using the CADPAC suite of programs.[28] At the SCF level we were able to use the full point group symmetry. However, at the MP2 level we could only employ the subgroup C_{2v} for both C_{4v} square-pyramidal $C_5H_5^+$ and the D_{2d} $B_8H_8^{2-}$ dodecadeltahedron. The magnitude of the maximum component of the Cartesian gradient was reduced to 10^{-5} hartree bohr^{-1}, except in the case of D_{2d} $B_8H_8^{2-}$ at the MP2/DZ level, for which the surface was found to be very flat and a tolerance of 10^{-4} was used. Analytic force constant matrices obtained from a lower level of theory were used to ensure rapid convergence. Three basis sets were considered: minimal STO-3G for preliminary investigations, double-ζ,[29] and double-ζ plus polarization (DZP) with a single set of p-functions on the hydrogen atoms (exponent 1.0) and a single set of d-functions on the boron and carbon atoms (exponents 0.7 and 0.8, respectively). The DZP basis therefore comprised 105 basis functions for $C_5H_5^+$ and 168 for $B_8H_8^{2-}$, the largest that could reasonably be employed with current resources.

We expect that polarization functions are likely to be very important for a good description of the $B_8H_8^{2-}$ dianions. In addition, realization is growing that polarization functions with medium size exponents are important in a correlated calculation to account for correlation corrections from the valence electrons. The MP2 method is the least computationally expensive way of introducing the correlation energy available today.[30] We are justified in using it for the present systems because at each geometry in question a single reference configuration is dominant. Hence, a method which models dynamic electron correlation is appropriate. For highly accurate calculations it is now accepted that large basis sets are required, but a practical compromise must be made because at present disc-space requirements are prohibitive for MP2 gradient and analytic force constant calculations unless there is high symmetry. Our physical interest is in surface topology, and for these 10- and 16-atom clusters frequencies must be calculated by analytic methods. Currently it is not practical to obtain these in calculations with more than about 120 basis functions. Hence we were not able to check the frequencies of the two $B_8H_8^{2-}$ structures at the MP2/DZP level or D_{2d} $B_8H_8^{2-}$ at the MP2/DZ level; however, the advent of fully direct algorithms in the future will help to alleviate such difficulties. For $B_8H_8^{2-}$ at the MP2 level we hope that the surface topology will not change with the inclusion of polarization functions; the change in the barrier height will be discussed.

The energies, rearrangement barriers, and Hessian indices of the four geometries, two for each of the $B_8H_8^{2-}$ and $C_5H_5^+$, are

(18) Dewar, M. J. S.; McKee, M. L. *Inorg. Chem.* **1978**, *17*, 1569.
(19) Kleier, D. A.; Lipscomb, W. N. *Inorg. Chem.* **1979**, *18*, 1312.
(20) Fuller, D. J.; Kepert, D. L. *Inorg. Chem.* **1982**, *21*, 163. Fuller, D. J.; Kepert, D. L. *Polyhedron* **1982**, *21*, 163.
(21) Wales, D. J. *J. Chem. Phys.* **1989**, *91*, 7002. Braier, P. A.; Berry, R. S.; Wales, D. J. *J. Chem. Phys.* **1990**, *93*, 8745. Wales, D. J. *J. Chem. Soc., Faraday Trans.* **1990**, *86*, 3505. Wales, D. J. *J. Am. Chem. Soc.* **1990**, *112*, 7908. Davis, H. L.; Wales, D. J.; Berry, R. S. *J. Chem. Phys.* **1990**, *92*, 4308.
(22) Wales, D. J.; Berry, R. S. *J. Chem. Phys.* **1990**, *92*, 4283.
(23) Muetterties, E. L.; Wiersema, R. J.; Hawthorne, M. F. *J. Am. Chem. Soc.* **1973**, *95*, 7520.
(24) Stohrer, W.-D.; Hoffmann, R. *J. Am. Chem. Soc.* **1972**, *94*, 1661.
(25) Bouman, T. D.; Duncan, C. D.; Trindle, C. *Int. J. Quant. Chem.* **1977**, *11*, 399.
(26) Longuet-Higgins, H. C. *Mol. Phys.* **1963**, *6*, 445.
(27) Murrell, J. H.; Laidler, K. J. *Trans. Faraday Soc.* **1968**, *64*, 371.
(28) Amos, R. D.; Rice, J. E. *CADPAC: the Cambridge Analytic Derivatives Package*; Cambridge, 1987; Issue 4.0.
(29) Dunning, T. H. *J. Chem. Phys.* **1970**, *53*, 2823. Huzinaga, S. *J. Chem. Phys.* **1965**, *42*, 1293.
(30) Møller, C.; Plesset, M. S. *Phys. Rev.* **1934**, *46*, 618.
(31) These plots were produced using Mathematica 2.0 © Wolfram Research Inc.

Table I. Energies, Rearrangement Barriers and Hessian Indices (Square Brackets) for $B_8H_8^{2-}$ and $C_5H_5^+$ at Various Levels of Theory[a]

(a) $B_8H_8^{2-}$

D_{2d} Dodecadeltahedron and C_{2v} Bicapped Trigonal Prism

	$B_8H_8^{2-}$			
method/basis	D_{2d}	C_{2v}	ΔE	ΔE_c
SCF/STO-3G	−199.383 413 [0]	−199.371 060 [1]	32.4	30.6
SCF/DZ	−201.923 392 [0]	−201.920 024 [0]	8.8	8.5
SCF/DZP	−202.028 506 [0]	−202.022 888 [1]	14.7	13.7
MP2/DZ	−202.521 842 [*b*]	−202.515 659 [1]	16.2	
MP2/DZP	−202.912 870 [*b*]	−202.902 185 [*b*]	28.1	

(b) $C_5H_5^+$

C_{4v} Square-Based Pyramid and C_{2v} Bridged Structure

	$C_5H_5^+$			
method/basis	C_{4v}	C_{2v}	ΔE	ΔE_c
SCF/STO-3G	−189.561 370 [0]	−189.529 347 [1]	84.1	81.3
SCF/DZ	−191.749 503 [0]	−191.725 302 [1]	63.5	58.6
SCF/DZP	−191.896 783 [0]	−191.856 508 [1]	105.7	98.4
MP2/DZ	−192.228 462 [0]	−192.196 141 [2]	84.9	74.3
MP2/DZP	−192.605 420 [0]	−192.557 294 [1]	126.4	116.8

[a] ΔE are the barriers in kJ mol^{-1}, ΔE_c are the barriers when the zero-point-energy corrections are included; the energies in the other columns are in hartrees. [b] Frequencies not calculated.

reported in Table I. The zero-point-energy corrections to the barriers neglect all imaginary frequencies. The MP2 contributions to the energies and barriers are given in Table II, all the frequencies are collected for $B_8H_8^{2-}$ in Table III and for $C_5H_5^+$ in Table IV, and some geometrical parameters are compared with experiment in Table V for $B_8H_8^{2-}$. For both molecules the proposed structures are indeed transition states, except for $C_5H_5^+$ at the MP2/DZ level, where the C_{2v} geometry has Hessian index 2, and $B_8H_8^{2-}$ at the SCF/DZ level, where the C_{2v} structure is a minimum. *The mechanisms are illustrated in Figures 3–5.*

The SDDS process (Figures 3 and 4) is equivalent to the rearrangement first proposed by Stohrer and Hoffmann.[24] Bouman et al. identify what appears to be the same motion as the one associated with the imaginary frequency of greatest magnitude in their calculations, but they interpret it as a Berry pseudorotation[32] which involves a quite different permutation of the vertices. The pseudorotation mechanism would correspond to a transition vector of A_2 symmetry, with no component on the edge-bridging carbon atom. In fact this mode represents the motion with the smallest real frequency for the C_{2v} structure in both the MP2/DZP and MP2/DZ calculations. We conjecture that Bouman et al. have plotted the normal mode corresponding to the SDDS process in their Figure 4c. Furthermore, the softest E mode of the C_{4v} minimum ranges between 342 and 546 cm^{-1} in frequency, and we see no evidence of the "large number of force constants near zero" reported by these authors. The normal mode associated with the other imaginary frequency for MP2/DZ C_{2v} $C_5H_5^+$ is sketched in Figure 6. It is significant that it does *not* correspond to either a pseudorotation or a "direct collapse" mechanism.[25]

It is clear from Table I that at both the SCF and MP2 levels of theory the effect of the polarization functions is to nearly double the barrier for the DSD process in $B_8H_8^{2-}$; this is also true when the zero-point correction is included. For the SDDS mechanism in $C_5H_5^+$ the effect is not as dramatic, but it is nevertheless apparent. The STO-3G results are inconsistent with this trend, presumably due to the inadequacies of this minimal basis. The MP2 corrections in $B_8H_8^{2-}$ show that polarization functions have a similar influence when electron correlation is included, whereas the contribution to the barrier in $C_5H_5^+$ is insignificant. This presumably reflects the importance of polarization functions for the anionic species.

The effect of the polarization functions upon the surface topology is a little disturbing. The $B_8H_8^{2-}$ D_{2d} structure is a minimum at each level of theory, but the C_{2v} structure is actually a minimum at the SCF DZ level. This is reversed again at the SCF/DZP level. Table V shows that the SCF/DZ geometry is significantly different from all the other levels of theory, although the ratio of the boron distances from the center of mass is actually closest to that reported experimentally.

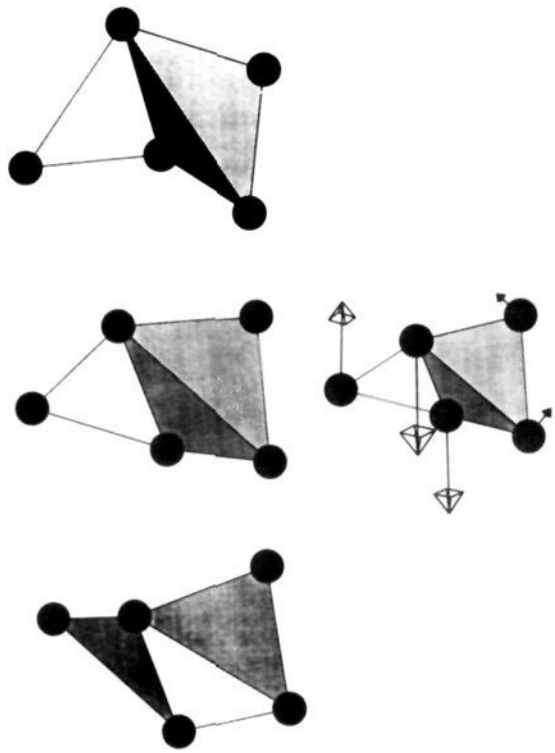

Figure 4. An alternative representation of the SDDS process in $C_5H_5^+$. The transition state is in the center, and the transition vector from the MP2/DZP calculations is plotted on the right. The geometries above and below the transition state were generated by adding (bottom) and subtracting (top) a suitable multiple of the transition vector to the transition-state geometry.[31]

For $C_5H_5^+$ the C_{2v} structure is a transition state at every level of theory except MP2/DZ, where its Hessian index is 2, i.e. there are two negative Hessian eigenvalues in addition to the six zeros. Although the second imaginary frequency is small in magnitude, it cannot be ignored, and it may be regarded as an artefact of a substantially incomplete basis. There is probably a second type of minimum at this level of theory.

The effect of electron correlation is greater for $B_8H_8^{2-}$ than for $C_5H_5^+$. For any given basis set the barrier to the DSD or SDDS process is approximately doubled in the former and increases only some 20–30% for the latter. The effect on the surface topology, however, is less dramatic than the effect of the polarization functions, so we can be fairly certain that dynamic correlation plays a less important role in an accurate description of these systems. Certainly the $B_8H_8^{2-}$ potential energy surface remains flatter in the region of the stationary points than that of $C_5H_5^+$ at both the SCF and MP2 levels, and the curvature increases when electron correlation is included in both cases. This is in line with the associated increase in the barrier heights. Finally, we note that the correlation energy itself increases by some 40–50% from the DZ to the DZP level in each system.

IV. Group Theory

In this section we briefly analyze the permutational symmetry of the SDDS mechanism. (The implications of the DSD mechanism for $B_8H_8^{2-}$ have been largely worked out before.[33]) We shall use a terminology recently described elsewhere[34] in which

(32) Berry, R. S. *J. Chem. Phys.* **1960**, *32*, 933.

(33) Gimarc, B. M.; Ott, J. J. In *Proceedings of the Conference on Graph Theory and Topology in Chemistry*; King, R. B., Ed.; Elsevier: Athens, Georgia, 1987.

Table II. Electron Correlation Contributions to the Energies and Rearrangement Barriers in the MP2 Approximation[a]

	$B_8H_8^{2-}$			$C_5H_5^+$		
method/basis	D_{2d}	C_{2v}	ΔE	C_{4v}	C_{2v}	ΔE
MP2/DZ	−0.600 775	−0.598 349	6.4	−0.487 170	−0.480 059	18.7
MP2/DZP	−0.886 072	−0.881 936	10.9	−0.710 443	−0.703 073	19.4

[a] ΔE are the contributions to the barriers in kJ mol^{-1}; the energies in the other columns are in hartrees.

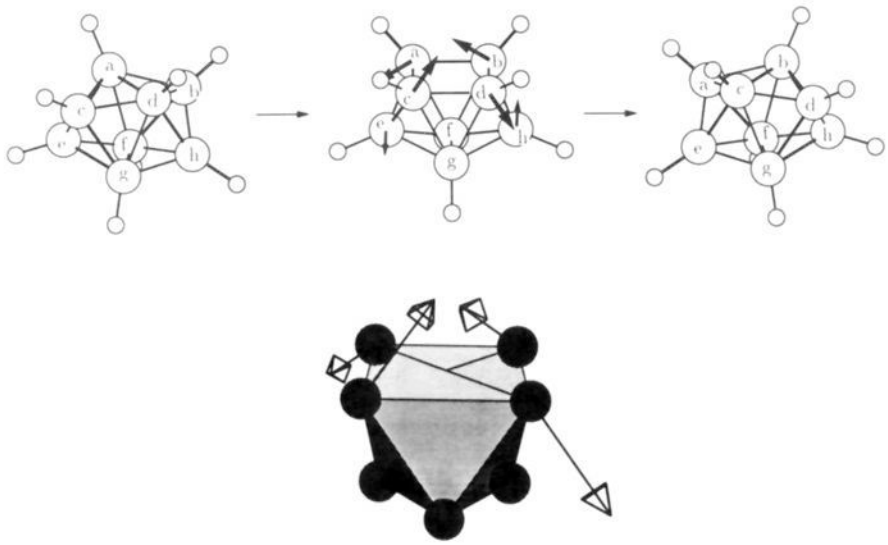

Figure 5. Mechanism of the DSD process in $B_8H_8^{2-}$. The transition vector corresponding to the normal mode with the imaginary frequency has been sketched for the transition state. Below this is an alternative representation of the transition state with the MP2/DZ transition vector superimposed.[31]

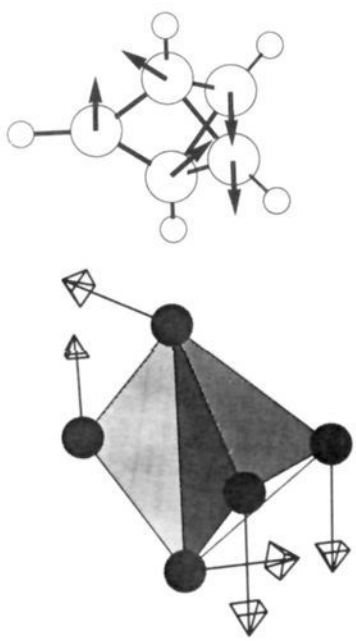

Figure 6. Two representations of the normal mode displacements corresponding to the imaginary frequency of 77i in C_{2v} $C_5H_5^+$ at the MP2/DZ level. The vectors are accurately plotted in the bottom view,[31] which is tilted somewhat relative to the view above it.

a *structure* specifies a particular geometry and has a number of *versions* distinguished from one another by the arrangement of atom labels. The correct symmetry group to use to describe isomerization reactions is the Molecular Symmetry (MS) group of Longuet-Higgins[26] and Bunker.[35] Boumann et al. were probably the first to use this group outside the field of spectroscopy, but, as we will explain, they have arrived at some incorrect conclusions concerning this reaction. The issue is to determine whether all the versions of the square-based pyramid may be accessed through the SDDS mechanism, and to demonstrate that the C_{2v} transition state is consistent with a group theoretical description of this rearrangement.

Bouman et al. state that the Stohrer–Hoffmann (SDDS) mechanism cannot lead to all five carbon atoms becoming equivalent. Again this contradicts Stohrer and Hoffmann,[24] who claim to have produced a complete, closed reaction graph for the 30 versions of the C_{4v} square-based pyramid. Here again we find in favor of Stohrer and Hoffmann's original conclusions. The problem arises because Bouman et al. classify the SDDS mechanism as a permutation corresponding to (aed) in our Figure 2. This permutation belongs to the class $(1^2, 3)$ in $\mathcal{S}_5$, the permutation group of five objects. Because the character of operations in the class $(1^2, 3)$ for the totally antisymmetric irreducible representation of this group is not minus one, they conclude that this mechanism could not lead to all five vertices becoming equivalent. The error in this analysis comes from the choice of the permutation (aed) to represent the SDDS mechanism. As we have explained elsewhere,[34] this choice involves ambiguity because one may combine the (aed) permutation with symmetry operations of the square-based pyramid such as (abec) (Figure 2). In fact,[34] the correct generating operation must be self-inverse so that it is a symmetry operation of the transition state. Consequently the operation can contain no permutations of cycle 3 or more, but it may contain the inversion of all particle coordinates, E^*. As we can see from Figure 3, which shows the same versions as Figure 2, in this case we may choose either $(de)^*$ or (de)(bc). The transition vector at the transition state is, of course, antisymmetric with respect to these two operations, corresponding to motions that interchange reactants and products, as required by the McIver–Stanton rules.[36]

We have verified that the reaction graph for the 30 versions of the C_{4v} structure is indeed closed for this mechanism. This means that if the SDDS mechanism is feasible[26] then the effective molecular symmetry group is the complete nuclear permuta-

(34) Bone, R. G. A.; Rowlands, T. W.; Handy, N. C.; Stone, A. J. *Mol. Phys.* **1991**, *72*, 33.

(35) Bunker, P. R. *Molecular Symmetry and Spectroscopy*; Academic Press: New York, 1979.

(36) McIver, J. W.; Stanton, R. E. *J. Am. Chem. Soc.* **1972**, *94*, 8618. Stanton, R. E.; McIver, J. W. *J. Am. Chem. Soc.* **1975**, *97*, 3632.

Table III. Frequencies (cm^{-1}) of All the $B_8H_8^{2-}$ Optimized Geometries[a]

D_{2d}			C_{2v}			
SCF STO3G	SCF DZ	SCF DZP	SCF STO3G	SCF DZ	SCF DZP	MP2 DZ
394	**240**	**306**	172i	44	45i	89i
394	**240**	**306**	532	391	435	397
521	394	410	546	415	439	407
528	428	432	575	448	475	420
604	462	485	598	491	523	481
709	559	598	670	517	525	485
757	588	603	716	571	582	525
757	612	**636**	760	625	641	581
762	**616**	**636**	768	625	655	593
780	**616**	648	807	638	658	613
850	**665**	**678**	914	730	727	675
850	**665**	**678**	924	740	746	698
996	788	**787**	950	746	751	701
996	**792**	**787**	966	760	762	708
1009	**792**	788	1003	791	799	742
1027	810	804	1007	804	805	752
1045	839	840	1042	825	831	773
1055	852	860	1052	838	842	784
1067	853	868	1063	853	871	803
1102	879	896	1067	871	876	809
1121	**916**	**926**	1100	889	898	820
1141	**916**	**926**	1129	908	917	827
1147	923	927	1142	910	921	840
1147	928	933	1151	921	940	844
1152	930	934	1159	926	941	862
1162	**939**	**954**	1159	949	962	872
1162	**939**	**954**	1196	953	967	884
1236	**984**	**981**	1225	986	986	905
1245	**984**	**981**	1253	994	988	908
1245	984	993	1256	1003	1018	916
1317	**1065**	**1072**	1283	1018	1030	927
1340	**1065**	**1072**	1359	1085	1099	997
1340	1076	1104	1373	1109	1124	1015
1461	1163	1192	1434	1133	1159	1049
3120	2528	2489	3097	2482	2463	2425
3127	**2530**	**2497**	3102	2492	2473	2435
3127	**2530**	**2497**	3110	2506	2483	2444
3133	2534	2501	3121	2524	2500	2463
3146	**2554**	**2522**	3144	2559	2524	2486
3146	**2554**	**2522**	3148	2569	2527	2492
3161	2567	2541	3165	2573	2546	2526
3176	2614	2577	3178	2621	2581	2549

[a] Degenerate pairs in boldface.

tion-inversion (CNPI) group. To prove this concisely we need only give the sequence of operations that results in pairwise exchange of two equatorial atoms and an equatorial atom with the axial atom for the square-based pyramid. The motion between two adjacent versions on the reaction graph interchanges the apical atom with one at the base; exchange of two neighboring basal atoms may be achieved in three steps, e.g. (bd) = (ec)*(ca)*(ae)*, where (ae)* is the first operation and (ec)* is the last and our labels are for the "reactant" square-based pyramid in Figure 2. The exchange of an atom in the equator with that at the apex may be achieved in four steps, e.g. (ae) = (ac)*(cd)*(db)*(be)*. We also agree with Stohrer and Hoffmann that five steps are needed to interconvert enantiomers, which are those versions related by the E^* inversion operation.[34] Clearly, when using generators of the type (de)*, an odd number of steps are required to leave us with an overall inversion; enantiomers are in fact related by the interchange of opposite equatorial vertices. This class of generator cannot effect such a swap in three steps; however, the sequence (bc) = (ec)*(ca)*(ab)*(bd)*(de)* does the trick.

It has also been shown[34] that the collection of operations comprising an MS group relates not only the versions of the equilibrium structure to one another but also those of any structure on the paths which connect them. Consequently if the order of the point group of any structure is h, and there are n distinct versions of that structure (connected by surmountable barriers), then the order of the MS group is nh. The order of the point group

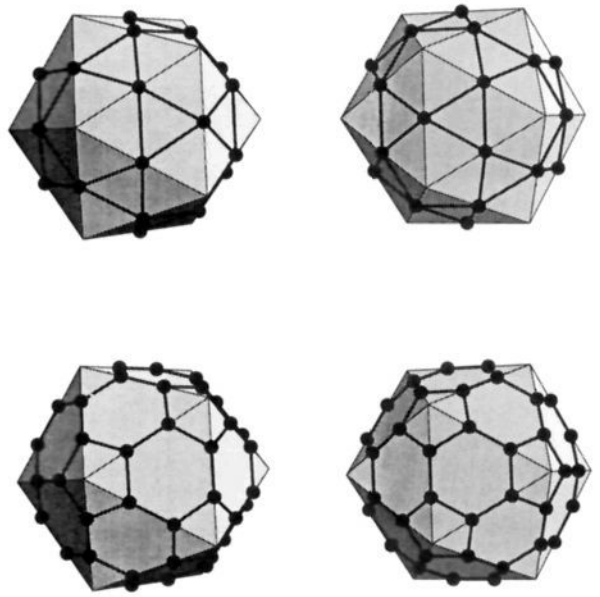

Figure 7. Geometrical interpretation of the tunnelling states for the rearrangement of C_{4v} $C_5H_5^+$ by the SDDS mechanism.[31] Top: Two views of the icosidodecahedron superimposed on an icosahedron, of which it is the edge dual. The black vertices represent distinct versions of the square-based pyramid, but the edges between them do NOT represent the transition states. Bottom: Two views of the truncated icosahedron superimposed on an icosahedron. Here, the black vertices represent distinct versions of the C_{2v} transition state. The edges are not physically meaningful in this context.

C_{4v} is 8 and that of C_{2v} is 4, so there must be $(8 \times 30)/4 = 60$ versions of the transition state involved. This is consistent with Stohrer and Hoffmann's discussion[24] and also the reaction graph we have derived.

Following the methods outlined by Bunker[35] we may correlate the ground vibrational state in one version of the minimum with the levels of the wave functions spanned by the 30 minima. We label the irreducible representations of the CNPI group $\mathcal{S}_5^* = (E,E^*) \otimes \mathcal{S}_5$ as Γ_{1-7} according to those of $\mathcal{S}_5$ following Hamermesh,[37] *with an additional superscript ± to denote the parity under* E^*. Using "upward-correlation"[38] we obtain the symmetries of the levels. The wave functions spanning the 30 minima may be found directly by diagonalizing the adjacency matrix of the reaction graph.[39] If x is the value of the matrix element which couples two versions of the square-based pyramid that are connected by a single step (and the other elements are assumed to be zero), we find the following states and energies (with degeneracies in parentheses):

$\Gamma_1^+(1)$	$\Gamma_4^-(4)$	$\Gamma_5^+(5)$	$\Gamma_6^-(5)$	$\Gamma_3^+(4)$	$\Gamma_6^+(5)$	$\Gamma_7^-(6)$
$4x$	$3x$	$2x$	0	$-x$	$-2x$	$-2x$

In fact, it is not possible to determine which of the five-degenerate irreducible representations at energies of $-2x$ and $2x$ is Γ_5 and which is Γ_6. The accidental degeneracy observed at $-2x$ is typical of highly symmetrical simpel "Hückel" problems. The eigenvalue of $4x$ simply reflects the connectivity of the reaction graph[5]—it corresponds to the totally in-phase linear combination.

The structure of the CNPI group $\mathcal{S}_5^*$ contains a hidden symmetry which may be used to provide a geometrical interpretation of the potential surface. First we note that the alternating group of order 5, $\mathcal{A}_5$, is a subgroup of $\mathcal{S}_5$ and is isomorphic to the point group I. Similarly, I_h is isomorphic to $\mathcal{A}_5^* = (E,E^*) \otimes \mathcal{A}_5$ which is a subgroup of $\mathcal{S}_5^*$, where the g/u parity in I_h correlates with the parity under E^* in $\mathcal{A}_5^*$ and $\mathcal{S}_5^*$. This means that the tunnelling states of the minima span a 30-dimensional representation of I_h, and the tunnelling states of the transition states span a

(37) Hamermesh, M. *Group Theory and its Application to Physical Problems*; Pergamon: New York, 1962.
(38) Watson, J. K. G. *Can. J. Phys.* **1965**, *43*, 1996.
(39) Bone, R. G. A. Ph.D. Thesis, Cambridge University, 1992.

Table IV. Frequencies (cm^{-1}) of All the $C_5H_5^+$ Optimized Geometries[a]

C_{4v}					C_{2v}				
SCF STO3G	SCF DZ	SCF DZP	MP2 DZ	MP2 DZP	SCF STO3G	SCF DZ	SCF DZP	MP2 DZ	MP2 DZP
487	**344**	**517**	**342**	**546**	397i	378i	464i	451i	525i
487	**344**	**517**	**342**	**546**	776	641	683	77i	372
720	619	686	500	609	930	659	683	147	503
939	**899**	**872**	**792**	**801**	948	835	837	676	750
939	**899**	**872**	**792**	**801**	972	842	870	723	779
964	900	907	794	830	999	905	901	805	826
1078	**1047**	1051	911	943	1000	937	907	808	835
1079	**1047**	**1056**	**931**	**970**	1028	940	946	813	866
1079	1058	**1056**	**931**	**970**	1042	995	987	885	868
1104	1087	1077	1003	1012	1128	1080	1032	925	952
1177	**1152**	**1137**	**1019**	**1038**	1140	1105	1094	931	967
1177	**1152**	**1137**	**1019**	**1038**	1189	1116	1104	956	980
1182	1166	1139	1053	1048	1197	1130	1118	1027	1045
1296	1309	1286	1134	1192	1287	1187	1188	1054	1090
1427	1310	1352	1183	1222	1299	1207	1207	1077	1118
1482	1342	1373	1194	1283	1315	1309	1290	1171	1195
1529	1372	1427	1225	1337	1458	1374	1411	1293	1378
1627	**1498**	**1536**	**1330**	**1415**	1580	1490	1531	1377	1455
1627	**1498**	**1536**	**1330**	**1415**	1708	1570	1624	1427	1523
3722	3512	3456	3291	3333	3600	3423	3369	3218	3242
3736	**3520**	**3467**	**3306**	**3347**	3736	3521	3466	3314	3345
3736	**3520**	**3467**	**3306**	**3347**	3758	3526	3467	3320	3362
3748	3536	3479	3322	3360	3764	3527	3468	3322	3362
3783	3560	3498	3343	3381	3797	3563	3501	3356	3385

[a] Degenerate pairs in boldface.

Table V. The Two Distances (Å) of the Boron Atoms from the Center of Mass in D_{2d} $B_8H_8^{2-}$

method/basis	r_{B1}	r_{B2}	r_{B1}/r_{B2}
SCF/STO-3G	1.521	1.292	1.177
SCF/DZ	1.575	1.360	1.159
SCF/DZP	1.570	1.329	1.182
MP2/DZ	1.604	1.358	1.182
MP2/DZP	1.573	1.302	1.208
experiment[43]	1.508	1.315	1.15 ± 0.02

60-dimensional representation. In fact, the above representations are simply those spanned by the 30 and 60 orbits of I_h which correspond to the vertices of an icosidodecahedron and of a truncated icosahedron, respectively. (An orbit of a point group is a complete set of symmetry equivalent points.[40]) These structures are shown in Figure 7; the icosidodecahedron is the face dual of the icosahedron and of the dodecahedron—the truncated icosahedron has recently become ubiquitous in the chemical literature.[41] The two representations are easily formed and reduced:

$$\Gamma_{30} \cong A_g \oplus G_g \oplus G_u \oplus 2H_g \oplus H_u \oplus T_{1u} \oplus T_{2u}$$

$$\Gamma_{60} \cong A_g \oplus T_{1g} \oplus T_{2g} \oplus 2G_g \oplus 3H_g \oplus 2T_{1u} \oplus 2T_{2u} \oplus 2G_u \oplus 2H_u \quad (1)$$

Descent-in-symmetry from $\mathcal{S}_5^*$ now enables us to deduce the tunnelling energy levels. We gave the result for Γ_{30} above (note that $T_{1u} \oplus T_{2u}$ correlates with the 6-fold degenerate irreducible representation Γ_7^-); for Γ_{60} we obtain

$$\Gamma_{60} \cong \Gamma_1^+(1) \oplus \Gamma_7^+(6) \oplus 2\Gamma_{3/4}^+(4) \oplus 3\Gamma_{5/6}^+(5) \oplus 2\Gamma_7^-(6) \oplus 2\Gamma_{3/4}^-(4) \oplus 2\Gamma_{5/6}^-(5) \quad (2)$$

We have labeled these $\mathcal{S}_5^*$ irreducible representations as before; however, the parity under an operation in the class (2, 1^3), such as (ab), is not known because we have used descent-in-symmetry rather than Watson's "upwards correlation". Hence we cannot distinguish between e.g. Γ_3 and Γ_4 both of which are 4-fold degenerate, without further calculation. However, the descent-in-symmetry approach is much faster and gives the correct pattern of degeneracies.

Therefore, although it is tempting to identify the 60 edges of the icosidodecahedron (Figure 7) with the 60 transition states, the connectivity of the reaction graph is actually much more complicated than this. Although both the minima and transition states may be represented separately as orbits of I_h, it is not possible to represent them simultaneously in this way. The complexity is apparent if we consider the 60 transition states, each of which must be linked to 6 others by 2 distinct minima. If the edges of the icosidodecahedron really reflected the connectivity of the reaction graph then we would be able to construct an approximate level diagram merely by node-counting[5] for the appropriate spherical harmonics with $L = 0, 1, 2$, etc. By descent-in-symmetry $L = 0$ corresponds to the A_g state in I_h with no nodes, $L = 1$ corresponds to T_{1u} with one nodal plane, $L = 2$ corresponds to H_g with two nodes, and so forth. However, the T_{1u} states actually lie at the opposite end of the spectrum from the A_g, indicating that the connectivity is much more complicated than this. The complete graph is available on request from the authors.

V. Conclusions

We have characterized the DSD mechanism for $B_8H_8^{2-}$ and the SDDS mechanism for $C_5H_5^+$ by ab initio calculations including polarization functions and correlation energy corrections at the MP2 level. In both cases we are able to confirm that the expected structures are indeed true transition states at most levels of theory, including the highest. Although the topologies of the potential energy surfaces are relatively insensitive to the basis set and electron correlation, the rearrangement barriers may change by up to a factor of 2. We have also deduced the effective molecular symmetry group for $C_5H_5^+$ when the SDDS mechanism is feasible. We conclude that this group is in fact the complete nuclear permutation-inversion (CNPI) group, in agreement with the original analysis of Stohrer and Hoffmann.

We also note that for both mechanisms studied in this paper the motion can be thought of as an initial perturbation along one component of a doubly degenerate vibrational mode. This leads to the required lowering of symmetry and also allows the connectivity of the reaction graph to be four at each minimum. If

(40) See e.g.: Coxeter, H. S. M. *Introduction to Geometry*, 2nd ed.; Wiley: New York, 1989.

(41) Kroto, H. W.; Heath, J. R.; O'Brien, S. C.; Curl, R. F.; Smalley, R. E. *Nature* **1985**, *318*, 162.

(42) ACES (Advanced Concepts in Electronic Structure)—An ab initio Program System, authored by Bartlett, R. J.; Purvis, G. D.; Fitzgerald, G. B.; Harrison, R. J.; Lee, Y. S.; Laidig, W. D.; Cole, S. J.; Trucks, G. W.; Magers, D. H.; Salter, E. A.; Sosa, C.; Rittby, M.; Pal, S.; Stanton, R. F.

(43) For the $Zn(NH_3)_4^{2+}B_8H_8^{2-}$ salt: Guggenberger, L. J. *Inorg. Chem.* **1969**, *8*, 2771.

the mode in question were nondegenerate then it would have to transform into plus or minus itself under any point group symmetry operation. Hence there could not be more than two versions of the transition state connected to any given minimum.

Acknowledgment. D.J.W. gratefully acknowledges Lloyd's of London for a Tercentenary Fellowship (1990-91) and the Royal Society for a University Research Fellowship (1991-). R.G.A.B. thanks Clare College, Cambridge, for financial assistance. Some of the SCF results confirm unpublished work performed in 1989 by D.J.W. and Prof. R. F. Stanton using the ACES package.[42] The group theoretical section of this paper benefitted greatly from discussions with Dr. G. K. Sankaran. Our calculations were made possible thanks to grants from the SERC and very generous allowances of disc space by the University of London Computer Centre.

Theoretical Studies of Spin-Forbidden Radiationless Decay in Polyatomic Systems: Insights from Recently Developed Computational Methods

David R. Yarkony

Contribution from the Department of Chemistry, The Johns Hopkins University, Baltimore, Maryland 21218. *Received January 2, 1992*

Abstract: We consider spin-forbidden radiationless decay of a bound electronic state which is metastable owing to a crossing with a dissociative potential energy surface of different spin-multiplicity. The minimum energy point on the spin-allowed surface of intersection of the bound and dissociative potential energy surfaces (the minimum energy crossing point) represents a key bottleneck along the minimum energy dissociation path, and frequently represents the transition state for this process. Thus the characterization of the minimum energy crossing point yields valuable mechanistic insights into this class of reactions, providing information concerning the feasibility of radiationless decay and the likely decomposition products. Traditional approaches for determining this point using multireference CI wave functions are computationally costly. However, a recently introduced algorithm, which uses analytic energy gradients and determines this point directly, that is without prior characterization of the surface of intersection, has reduced considerably the requisite computational effort. This algorithm is used to consider postulated spin-forbidden radiationless decay channels in tetrahedral N_4, $N_4(^1A_1) \rightarrow N_4(^3A'') \rightarrow N_2(X^1\Sigma_g^+) + N_2(A^3\Sigma_u^-)$ and in the methoxy cation, $CH_3O^+(^3A_2) \rightarrow CH_3O^+(^1A') \rightarrow HCO^+(X^1\Sigma^+) + H_2(X^1\Sigma_g^+)$. For the methoxy cation it is shown, using CI expansions as large as 2.5 million configuration state functions, that $\Delta E = 15.4$ kcal/mol, where ΔE is defined as the difference between the energy at minimum energy crossing structure and the energy at the minimum on the bound state potential energy surface. Thus the indicated reaction provides a low energy decomposition pathway. For tetrahedral N_4, ΔE for the indicated process is 28.2 kcal/mol which is half the barrier for the spin-allowed decay channel.

I. Introduction

In this work we consider systems in which the vibrational levels of a bound potential energy surface are rendered metastable by the spin-orbit induced coupling to a dissociative state of different spin-multiplicity. In a phenomenological sense, this process, spin-forbidden predissociation or spin-forbidden radiationless decay, is well understood. However, the computational treatment of this problem in polyatomic systems is particularly challenging. The first task is to establish the dissociation pathway (or pathways) which is (are) energetically accessible to the quasibound molecule. The minimum energy point on the spin-allowed surface of intersection of the two surfaces in question, the minimum energy crossing point, represents a key bottleneck along the minimum energy path[1] and is frequently the transition state for this pathway. Thus the determination of this point (i) provides the barrier for the decomposition pathway, or at least a lower bound if the true transition state lies elsewhere on the bound state surface, and (ii) can, particularly for a late or product channel minimum energy crossing point, establish the products of the radiationless decay process. Clearly then, the determination of this point provides essential information concerning the mechanism and feasibility of spin-forbidden radiationless decay and is a logical starting point for any treatment of this process.

The straightforward procedure that has been used in the past to locate the minimum energy point,[2] the indirect determination of this point, initially determines the crossing surface and then characterizes its minimum. This procedure is computationally costly since for a system with N internal degrees of freedom a crossing surface, or seam, of dimension $N-1$ must be determined and analyzed. Thus the determination of this point represents a computational bottleneck in the study of this class of processes. However, this bottleneck can be avoided. Fletcher[3] has shown that the minimum energy crossing point can be determined by a Lagrange multiplier constrained minimization procedure which determines this point directly, that is, without prior determination of the crossing surface itself. Implementations of this algorithm have been reported initially by Koga and Morokuma[4] based on SCF wave functions and more recently by the present author[5] using MCSCF/CI wave functions.

This work focuses on the use of this methodology to determine the feasibility of proposed spin-forbidden radiationless decay processes. This is the essential first step in a quantitative characterization of a predissociation or radiationless decay rate. The complete description, which is beyond the scope of the present work, requires (i) a more complete knowledge of the relevant potential energy surfaces, (ii) the spin-orbit induced coupling between these potential energy surfaces, and (iii) the solution of

(1) Kato, S.; Jaffe, R. L.; Komornicki, A.; Morokuma, K. *J. Chem. Phys.* **1983**, *78*, 4567.

(2) Alexander, M. H.; Werner, H.-J.; Hemmer, T.; Knowles, P. J. *J. Chem. Phys.* **1990**, *93*, 3307.

(3) Fletcher, R. *Practical Methods of Optimization*; John Wiley: New York, 1981.

(4) Koga, N.; Morokuma, K. *Chem. Phys. Lett.* **1985**, *119*, 371.

(5) Yarkony, D. R. *J. Chem. Phys.* **1990**, *92*, 2457.

0002-7863/92/1514-5406$03.00/0